Desalination and Water Treatment
www.deswater.com

doi: 10.5004/dwt.2018.22644

129 (2018) 207–215
October

A facile ternary molten salts method to synthesize magnesium borate ($Mg_2B_2O_5$) nanorods using desalinated concentrated seawater

Licong Wang*, Haihong Wu, Shubao Gao, Tao Li, Shaoyan Lu, Liang Wang, Xiping Huang

The Institute of Seawater Desalination and Multipurpose Utilization (SOA), Tianjin, 300192, China, Tel. +86 2287898172; emails: wanglicong@eyou.com (L. Wang), hongwhh@163.com (H. Wu), cranberriesgao@163.com (S. Gao), Bluewave0607@sina.com (T. Li), y4771558@163.com (S. Lu), Wl-bh@163.com (L. Wang), xipinghuang@163.com (X. Huang)

Received 20 October 2017; Accepted 19 June 2018

ABSTRACT

$Mg_2B_2O_5$ nanorods were synthesized in NaCl-KCl-Na_2SO_4 ternary molten salts using desalinated concentrated seawater. The products were characterized by X-ray diffraction, scanning electron microscopy, X-ray photoelectron spectroscopy (XPS), Fourier transform infrared spectrum (FT-IR) and Brunauer–Emmett–Teller (BET). The results showed that $Mg_2B_2O_5$ nanorods can be obtained at 780°C, the diameter was in the range of 100–150 nm and the length was more than 5 μm. XPS results confirmed that the molar ratio of each atom agreed with the stoichiometric composition of $Mg_2B_2O_5$. FT-IR showed that the structure of $Mg_2B_2O_5$ was composed of $B_{(3)}$-O and $B_{(4)}$-O units. The BET specific surface area of the sample calculated from N_2 isotherms was found to be 9.9408 m^2/g, the pore volume was 0.015 cm^3/g. The advantage of ternary molten salts method for synthesizing $Mg_2B_2O_5$ nanorods comparing with single molten salt method was briefly discussed.

Keywords: Magnesium borate; Nanorod; Ternary molten salts; Desalinated concentrated seawater

1. Introduction

In recent years, the morphology and size of materials have attracted the attention of the researchers because chemical and physical properties of materials had related to the micro-morphology and size [1]. One-dimensional (1D) nanostructure materials, such as nanowires, nanotubes, nanobelts, nanorods etc., have been the focus of intensive research owing to their great potential application [2].

As one of the remarkable ceramic materials, magnesium borates have been widely used to reduce the base oil friction coefficient owing to its excellent anti-wear and anti-corrosion properties [3,4]. It also has other potential applications, such as catalysts in the conversion of hydrocarbons [5,6], luminescent materials in cathode ray tube screens [7] and thermo-luminescence applications [8,9]. It is believed that 1D nanostructure magnesium borates may offer some outstanding properties compared with the bulk material.

With the development of 1D nanomaterials, magnesium borates 1D nanostructure has been synthesized with various methods. For example, $Mg_2B_2O_5$ nanowires [10] have been synthesized by the chemical vapor deposition at the temperature of 750°C–1,100°C, the diameter and the length of nanowires were 30–150 nm and 1–10 μm, respectively. $Mg_3B_2O_6$ nanobelts [11] have been synthesized by solid-state reaction at the temperature of 1,100°C and the nanobelts with the diameter of 100–300 nm and the length up to tens of micrometers. $Mg_3B_2O_6$ nanotubes [12] have been fabricated by atmosphere sintering and the nanobelts were with the diameter of 200–500 nm and length of 1–5 μm. $Mg_2B_2O_5$ nanorods [13] have been synthesized by solvent thermal method at the temperature of 400°C with the diameter of 100–150 nm and length of 1–5 μm. In addition, two-step processes such as template technology combined with the sintering method [3,14], sol-gel combined with the sintering method [15] have been also

* Corresponding author.

investigated for the purpose of fabricating 1D magnesium borates nanomaterials. However, these researches focus on the preparation technology without taking cost and practical applications into account, the problems such as complex equipments and continuous supply carrier gas, high energy consumption, multistep and rigorous experimental conditions still need to be solved.

The molten salt synthesis method has been a good traditional technology for preparing inorganic materials because of its simple instrumentation, low temperature and short holding time which make it actionable to carry out large-scale productions [16]. It was reported that single molten salt method has been used to synthesize $Mg_2B_2O_5$ nanorods [17] and nanowhiskers [18–20], with $MgCl_2 \bullet 6H_2O$ and $NaBH_4$, $MgCl_2 \bullet 6H_2O$, H_3BO_3 and NaOH as raw materials, respectively, and byproduct NaCl as molten salt. Binary molten salts method was also reported to synthesize $Mg_2B_2O_5$ nanowires with $MgCl_2 \bullet 6H_2O$, H_3BO_3, NaOH and boron nanoparticles as raw materials, NaCl and KCl as molten salts [21].

Multi-molten salts method can accelerate the diffusion speed of reaction constituents owing to its low viscosity as well as good fluidity. Furthermore, the crystal nucleation and growth environment are very stable, which could make the products generally possessing good crystallinity and uniform morphology.

Herein, it is worthwhile to develop a novel homogeneous precipitation combined with ternary molten salts process for preparing $Mg_2B_2O_5$ 1D nanomaterial using desalinated concentrated seawater, H_3BO_3 and NaOH. Desalinated concentrated seawater, abundant in $MgCl_2$, $MgSO_4$, NaCl and KCl, is a kind of high-quality liquid resource; direct discharge will cause the waste of resources. There are many advantages for preparing $Mg_2B_2O_5$ nanorods by ternary molten salts method using desalinated concentrated seawater. First, there is no need adding fresh water as well as re-dissolving magnesium source and molten salts in the homogeneous precipitation process, and both fresh water and energy resource are saved. Second, the generated byproduct Na_2SO_4, together with NaCl and KCl, which come from desalinated concentrated seawater, could act as the ternary molten salts in the homogeneous precipitation process. Last, the magnesium in concentrated seawater turns into high value products instead of the primary industrial raw materials such as $MgCl_2 \bullet 6H_2O$ and $MgSO_4 \bullet 7H_2O$, which is an innovation to the traditional technology of concentrated seawater utilization.

2. Experiment

2.1. Synthesis of $Mg_2B_2O_5$ nanorods with homogeneous precipitation combined with ternary molten salts

The concentration of $MgSO_4$, $MgCl_2$, KCl and NaCl in concentrated seawater was 0.44, 0.83, 0.24 and 3.59 M, respectively. A typical procedure, 28.3 g of H_3BO_3 was dissolved in 300 mL of concentrated seawater with continuous stirring to form a mixed solution, then 150 mL of 5 M NaOH solution was added dropwise into the mixed solution under vigorous mechanical stirring and precursor slurry was formed. At this homogeneous precipitation stage, $Mg_2(OH)_3Cl$, $Na_2B_4O_5(OH)_4 \bullet 8H_2O$ and Na_2SO_4 were formed. After drying the precursor slurry, a white powder was gained. The powder was then calcined in a muffle furnace at specific temperature for 2 h with a heating rate of 5°C/min. At this sintering stage, NaCl and KCl from the concentrated seawater and byproduct Na_2SO_4 acted as ternary flux. In order to gain $Mg_2B_2O_5$ nanorods, the mixture was washed with water to remove fluxes and then dried at 100°C for 5–6 h.

2.2. Synthesis of $Mg_2B_2O_5$ nanorods with single molten salts (NaCl) method

168.5 g $MgCl_2 \bullet 6H_2O$, 28.3 g H_3BO_3 and 104 g NaCl were dissolved in 300 mL of water with continuous stirring to form a mixed solution, then 150 mL of 5 M NaOH solution was added dropwise into the mixed solution under vigorous mechanical stirring and a precursor slurry was formed. After drying the precursor slurry, a white powder was gained and then calcined in a muffle furnace at specific temperature for 2 h with a heating rate of 5°C/min. In order to gain $Mg_2B_2O_5$ nanorods, the mixture was washed with water to remove fluxes and then dried at 100°C for 5–6 h.

2.3. Samples characterization

The phase structure of the as-prepared $Mg_2B_2O_5$ nanorods was identified by powder X-ray diffraction (XRD) on Japan D/MAX-2500 X-Ray diffractometer with a graphite-monochromatized Cu Kα radiation (1.5406 Å). The size and morphology of the as-prepared sample were observed by scanning electron microscopy (SEM, XL30, Philips). X-ray photoelectron spectroscopy (XPS) was recorded on the Perkin-ELMER PHI-1600ESCA X-ray photoelectron spectrometer with mon-chromatized MgKα as the radiation source operated at the power of 250W. The structure of the as-prepared samples was determined by the Fourier transform infrared spectrum (FT-IR). Nitrogen adsorption–desorption isotherms were measured with Micromeritics Tristar II (USA) analyzer at –196°C for measuring the pore sizes and specific surface areas of pristine SBA-15 and SBA-15/PA composite. Before measurement, the samples were degassed at 180°C in vacuum for more than 6 h. Their specific surface areas were calculated using the Brunauer–Emmett–Teller (BET) method. The pore diameters (D) were determined from the adsorption branch, according to Barrett–Joyner–Halenda (BJH) method. The total pore volume (V_t) was estimated from the amount adsorbed at the relative pressure (P/P_0) of 0.99.

3. Results and discussion

3.1. Structure analysis

Fig. 1 shows the XRD patterns of the powders calcined at different temperatures. All the diffraction peaks between 750°C and 780°C can be indexed as the triclinic $Mg_2B_2O_5$ (JCPDS 15-0537), no impurities such as Na_2SO_4, NaCl and KCl were detected in this pattern. With the increased temperatures, intensity of the diffraction peaks related to $Mg_2B_2O_5$ phase became sharper and stronger gradually. When the temperature increased to 780°C, the sharp diffraction peaks indicated that well-crystallized $Mg_2B_2O_5$ was formed, the

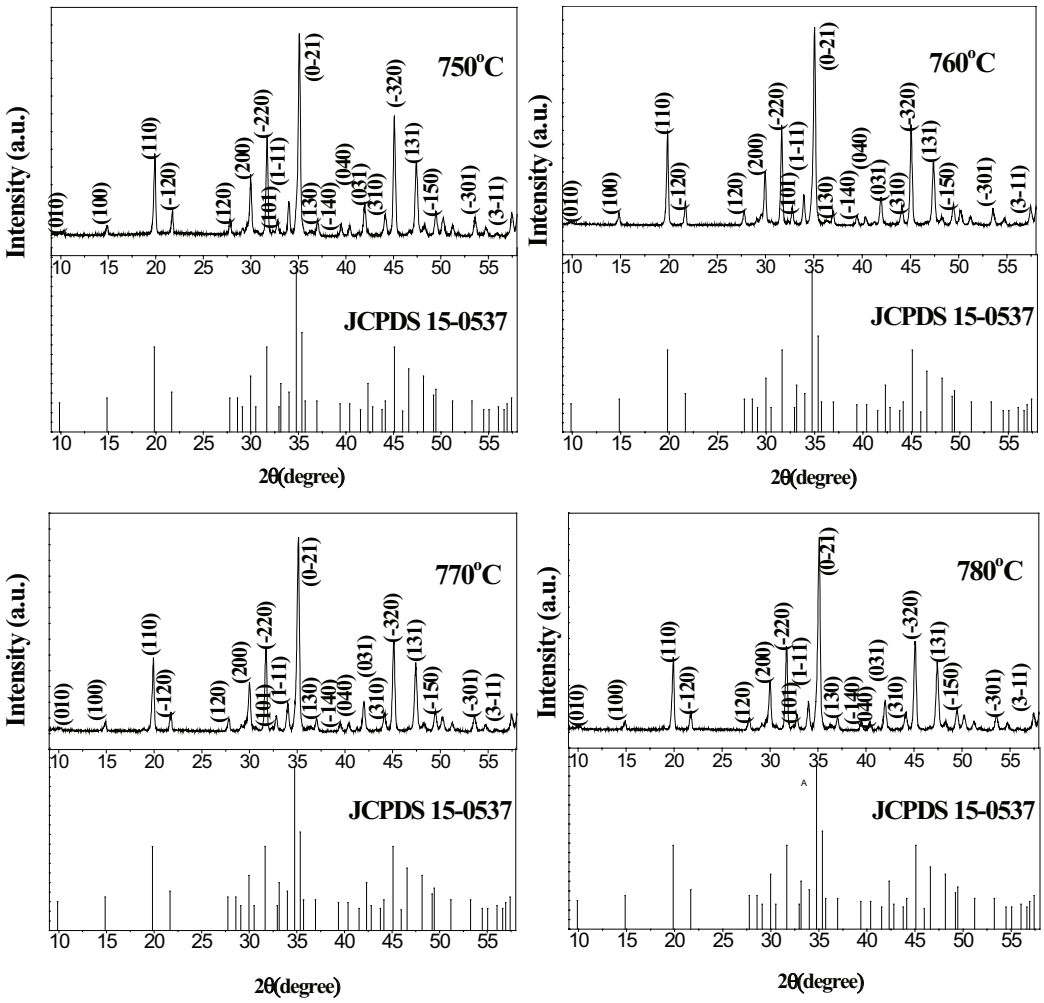

Fig. 1. XRD pattern of $Mg_2B_2O_5$ nanorods calcined at different temperatures by ternary molten salts method.

(0-21) lattice plane was preferred growth direction. In order to further confirm the crystallinity of the product, FWHM, crystal constants of $Mg_2B_2O_5$ at different temperatures were calculated and shown in Tables 1 and 2. It can be seen that with the temperature increased, crystal axis of crystal and crystal cell volume gradually reduced and when the calcined temperature was 780°C, all the parameters were almost the same to the theoretical value, which was in accord with the XRD results.

XRD principle and crystal growth theory show that if the sample to be tested is with good crystal, the diffraction peaks are narrow and their FWHM width are about 0.1°–0.2°, the crystal size of the sample is less than 300 nm. In this experiment, when the calcined temperatures are between 740°C and 780°C, the FWHM is reduced from 0.321° to 0.214°, and the diffraction peaks become shaper and sharper, the particle size increases accordingly. The results in this experiment prove those viewpoints.

3.2. Morphology analysis

Fig. 2 shows the morphology of the as-prepared samples calcined at different temperatures. It can be seen that banded and columnar fibrous materials were obtained but with

Table 1
FWHM and related data of $Mg_2B_2O_5$ at different calcinated temperatures

Calcinated temperature (°C)	Preferred lattice plane growth direction	FWHM (°)
750	0-21	0.321
760	0-21	0.245
770	0-21	0.228
780	0-21	0.214

Table 2
Crystal constants of $Mg_2B_2O_5$ at different calcinated temperatures

Calcinated temperature (°C)	a (Å)	b (Å)	c (Å)	V (Å^3)
750	6.1724	9.2345	3.1264	9.2345
760	6.1636	9.2318	3.1255	9.2318
770	6.1579	9.2254	3.1243	9.2254
780	6.1555	9.2208	3.1226	9.2208
Theoretical value	6.155	9.220	3.122	174.24

poor smoothness, in addition, there existed some irregular twin crystal, the diameter and length were in the range of 10–500 nm and 0.2–1 μm, respectively, at the temperature of 750°C (Fig. 2(a)). When the temperature increased to 760°C (Fig. 2(b)), rod-like and columnar fibrous materials appeared, the distribution of diameter and length became narrow; the diameter and length were in the range of 50–400 nm and 0.5–2 μm. As the temperature increased to 770°C (Fig. 2(c)), rod-like structure became gradually obviously and uniform; the diameter and length were in the range of 100–500 nm and 2–5 μm. When the temperature continuation increased to 780°C, the overall morphology of the sample indicated that a large amount of uniform nanorods with diameter of 100–150 nm and length over 5 μm can be seen.

The geometrical form and morphology of the $Mg_2B_2O_5$ nanorods are further elucidated by HRTEM, as shown in Fig. 3, which exhibits a typical morphology of nanorods and are in agreement with the above SEM findings. As can be seen in Fig. 3(a), the lattice spacings of 0.2995 and 0.2514 nm agree well with the [200] and [0-21] crystal planes of the triclinic $Mg_2B_2O_5$ (Fig. 3(b)). The electron diffraction pattern shown in Fig. 3(c) indicates that the nanorods are single crystal and (0-21) lattice plane was preferred growth direction, which is also supported by XRD result.

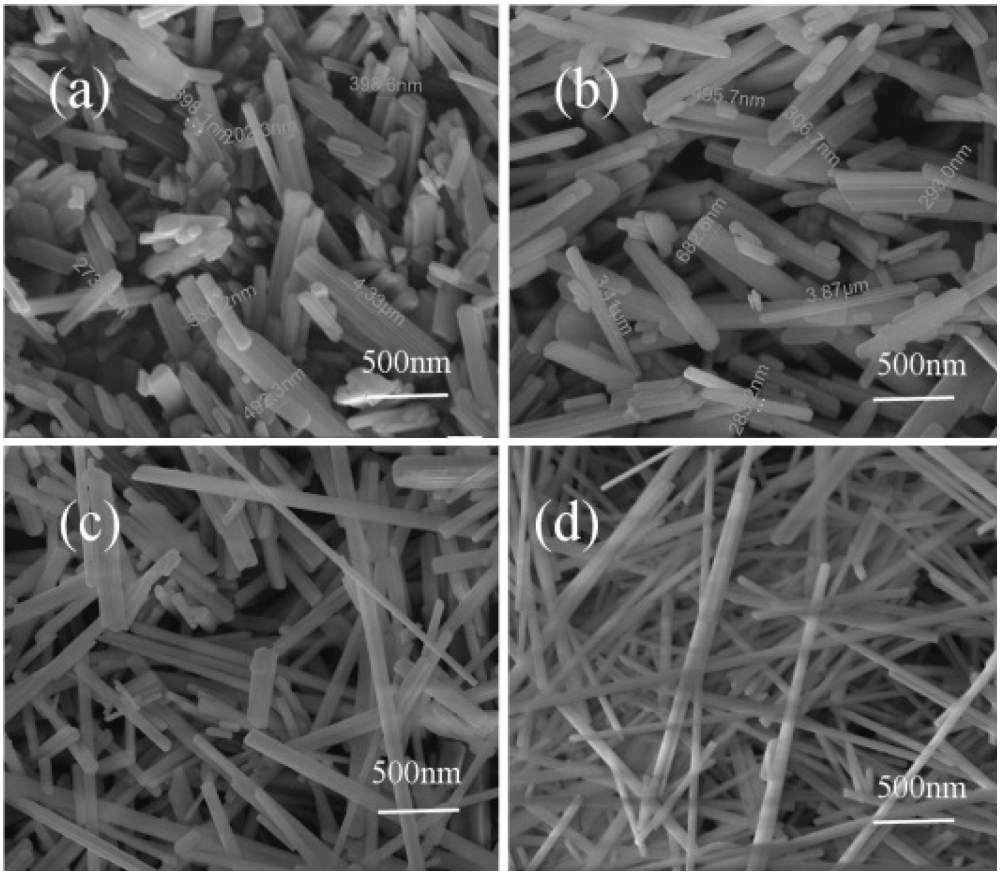

Fig. 2. SEM images of $Mg_2B_2O_5$ nanorods calcined at different temperatures by ternary molten salts method (a) 750°C, (b) 760°C, (c) 770°C and (d) 780°C.

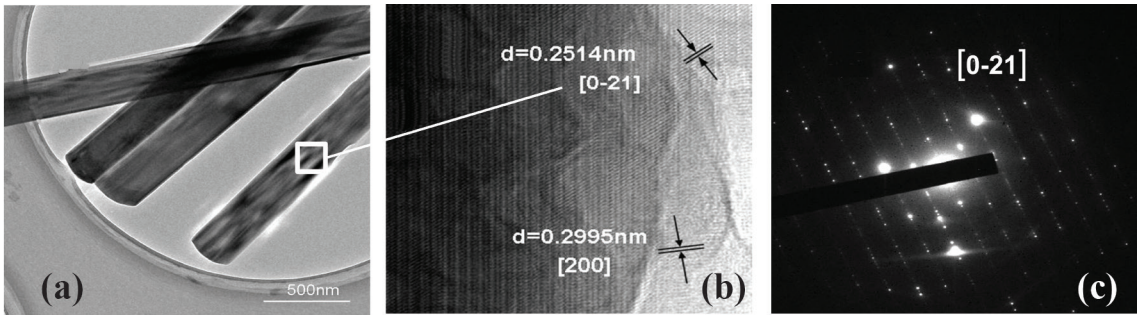

Fig. 3. HRTEM images of $Mg_2B_2O_5$ nanorod (a) micro-morphology of $Mg_2B_2O_5$ nanorod, (b) crystal planes of $Mg_2B_2O_5$ nanorod, (c) selected area electron diffraction (SAED) of $Mg_2B_2O_5$ nanorod.

3.3. XPS analysis

To further provide evidence for the as-prepared products, XPS was employed to analyze the elemental composition. Fig. 4(a) shows the survey spectra of the as-prepared nanorods. It can be seen that the surface consisted of Mg, B and O. Figs. 4(b)–(d) show that the binding energies of Mg 2p, B 1s and O 1s were 50.10, 192.10 and 531.45 eV, respectively, which was close to the binding energy of O^{2-} 1s, B^{3+} 1s and Mg^{2+} 2p. The quantification of O1s, B1s and Mg2p peaks confirmed that the atomic ratio of Mg:B:O = 1:1.01:2.51, which well agreed with the stoichiometric composition of $Mg_2B_2O_5$.

3.4. FT-IR analysis

Fig. 5 shows FT-IR spectrum of the as-prepared $Mg_2B_2O_5$ nanorods. The peak at 3,450 cm^{-1} was the O–H stretching of the absorbed water, the peak at 1,500 cm^{-1} was the asymmetric stretching of $B_{(3)}$-O, the peaks at 1,290 and 1,184 cm^{-1} were attributed to the in-plane bending of B–O–H. The peaks at 1,026 and 839 cm^{-1} were the asymmetric and symmetric stretching of $B_{(4)}$-O, respectively. And the peaks at 710 and 683 cm^{-1} were the out-of-plane bending of $B_{(3)}$-O, the peak at 613 cm^{-1} was symmetric pulse vibration of $[B_2O_5]^{4-}$, the peak at 540 cm^{-1} was the bending of $B_{(3)}$-O and $B_{(4)}$-O. The strongest vibrational peaks at 1,500 and 1,184 cm^{-1} were in agreement with the literature reports [19], FT-IR showed that the structure of $Mg_2B_2O_5$ is composed of $B_{(3)}$-O and $B_{(4)}$-O units.

3.5. BET analysis

It was reported that there existed pores in the one-dimension $Mg_2B_2O_5$ nanomaterials in the absence of flux agent but when the flux agent appeared, the pores disappeared [19]. So the nitrogen adsorption–desorption isotherms and porosity of the as-prepared $Mg_2B_2O_5$ nanorods were further investigated. As can be seen in Fig. 6, the nitrogen adsorption–desorption isotherms indicated that there existed weak force between N_2 and as-prepared $Mg_2B_2O_5$

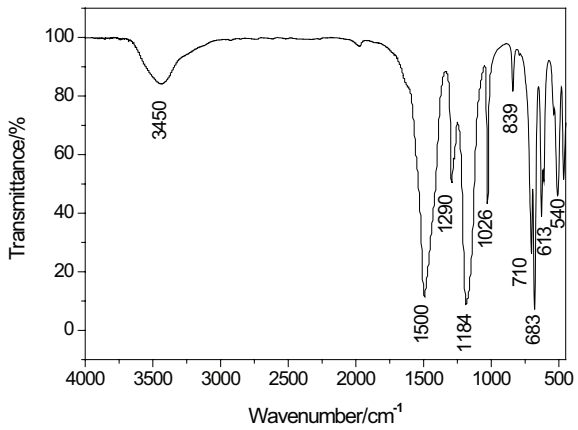

Fig. 5. FT-IR spectra of $Mg_2B_2O_5$ nanorods synthesized by ternary molten salts method.

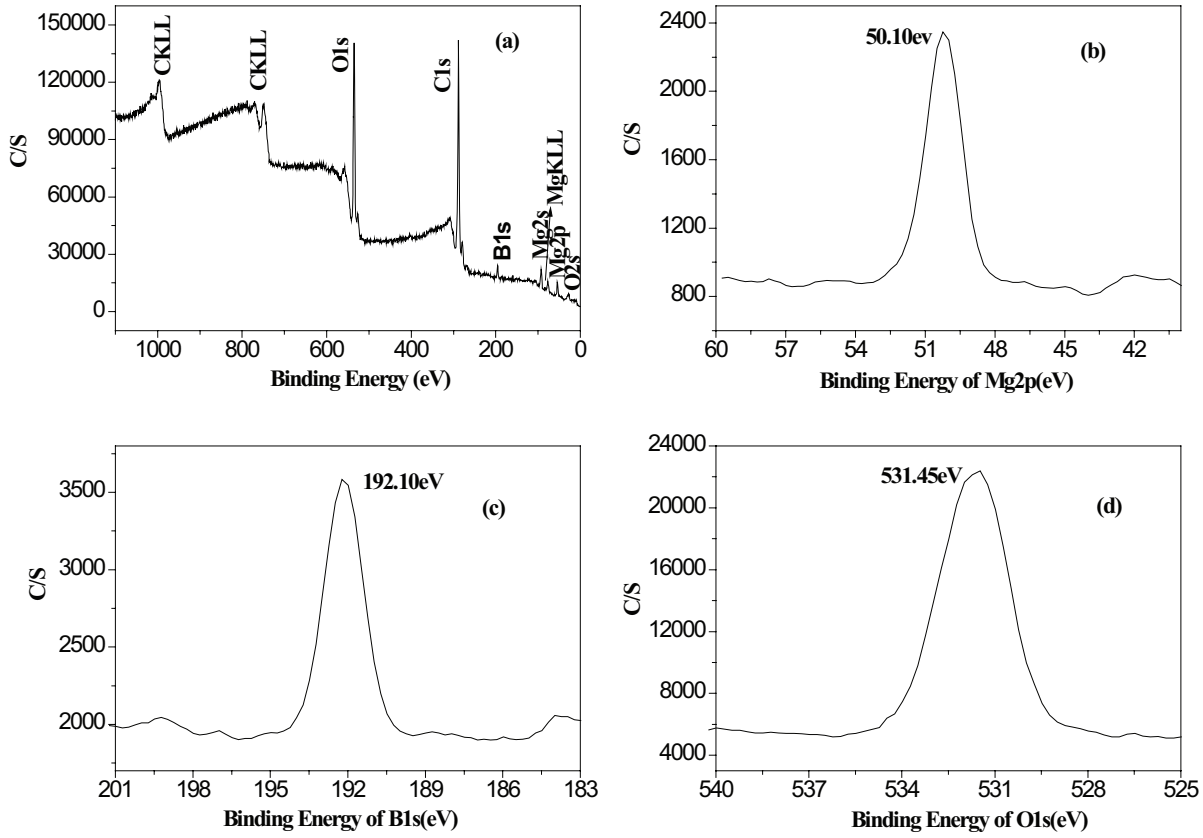

Fig. 4. XPS spectra of $Mg_2B_2O_5$ nanorods synthesized by ternary molten salts method. (a) survey spectra of the $Mg_2B_2O_5$ nanorods, (b) binding energy of Mg2p, (c) binding energy of B1s, (d) binding energy of O1s.

nanorods. This is probably due to the properties of boron and nitrogen. Nitrogen has lone pair of electrons and boron has vacant orbital, which may form weak covalent bond and led to nitrogen not to be completely desorbed from $Mg_2B_2O_5$. The BET specific surface area of the sample calculated from N_2 isotherms was found to be 9.9408 m^2/g and the pore volume is 0.015 cm^3/g, which implied that there is nearly no pore existed in the $Mg_2B_2O_5$ nanorods. The BET specific surface area is much smaller than the reported value which is 16.2 m^2/g [19]; this result further proved it was a kind of non-pore materials in the present developed method.

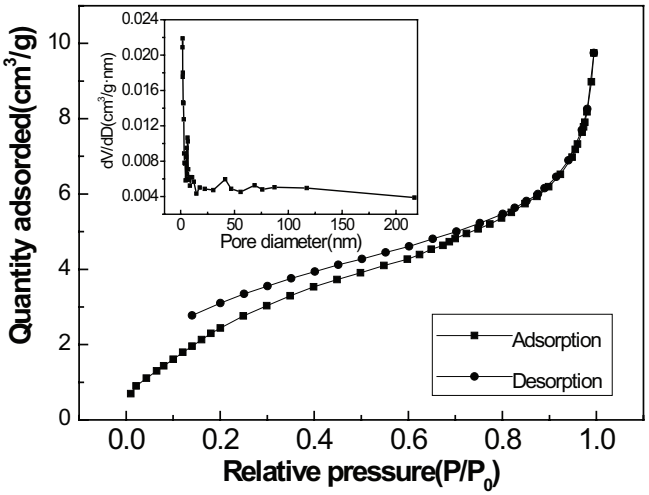

Fig. 6. Nitrogen sorption isotherms of $Mg_2B_2O_5$ nanorods synthesized by ternary molten salts method (the inset is the corresponding pore-size distribution).

3.6. Method comparison and advantage

In order to confirm the advantage of ternary molten salts process to synthesize $Mg_2B_2O_5$ nanorods, single molten salt (NaCl) method was also investigated. Fig. 7 shows the XRD patterns of the powders calcined at different temperatures. All the diffraction peaks between 750°C and 820°C can be indexed as the triclinic $Mg_2B_2O_5$ (JCPDS 15-0537), no impurities were detected. When the calcined temperature was 750°C, compared with other lattice plane, (110) lattice plane diffraction peak intensity was relatively strong. When the temperature increased to 770°C–820°C, (110) lattice plane diffraction peak intensity showed slow increase, but (200), (-220), (0-21), (021), (-320) and (131) lattice plane diffraction peaks intensity showed obvious decrease, the (110) lattice plane was preferred growth direction under the current preparation conditions.

The morphology of the samples calcined at different temperatures by single molten salt method is shown in Fig. 8. It can be seen that some irregular fibrous material with belt structure, columnar structure and needle-like structure formed at the temperature of 750°C (Fig. 8(a)). Diameter and length were in the range of 5–50 nm and 10–200 nm, respectively, the size was widely distributed and a small amount of grandular

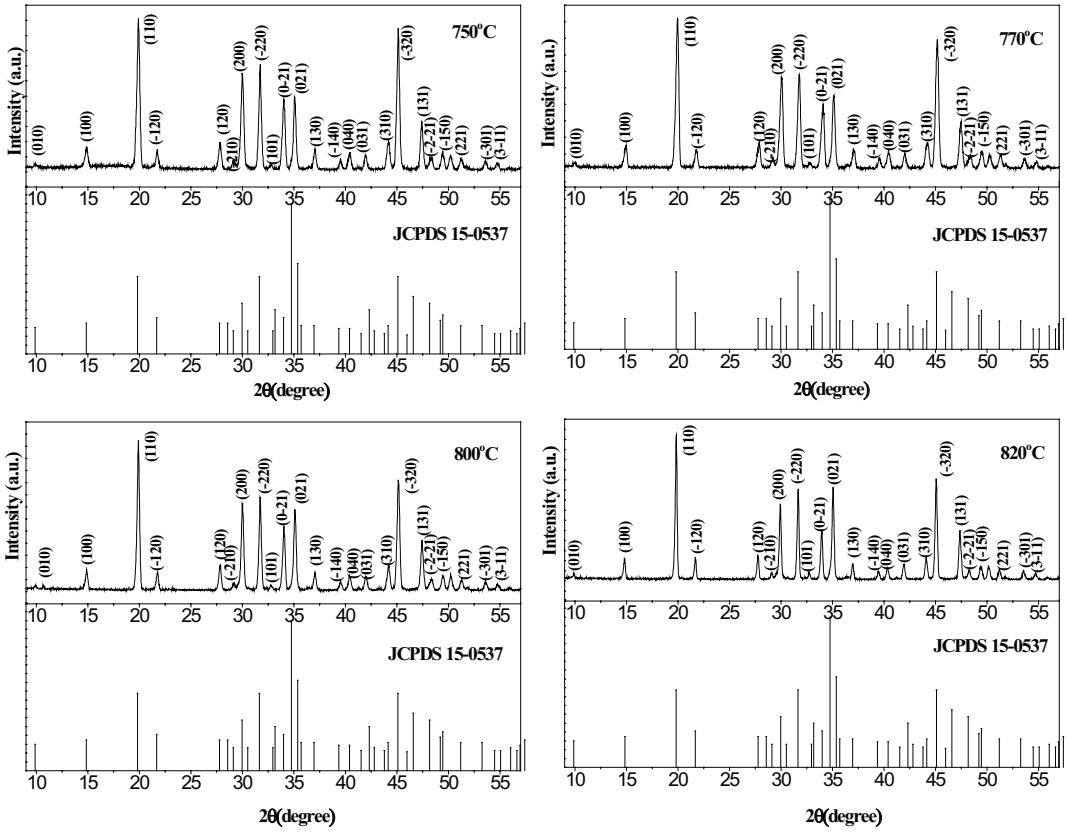

Fig. 7. XRD pattern of $Mg_2B_2O_5$ nanorods calcined at different temperatures by single molten salt method.

crystals particles attached on the fibrous materials. As the temperature increased to 770°C (Fig. 8(b)), the grandular crystals particles reduced greatly, and the diameter and length grew but not particularly significant, this is because NaCl is still not dissolved completely, the diffusion resistance of reactants in NaCl relatively greatly, which limits their coalescence and self-assembly into longer fibrous materials. As the temperature increased to 800°C (Fig. 8(c)), most NaCl were dissolved, and the reactants diffusion resistance became smaller because the temperature was very close to the melting point of sodium chloride, 802°C, both diameter and length grow more rapidly and fibrous structure became more and more significant. Grandular crystals particles and smaller size nanorods disappeared. As the temperature increases to 820°C, the morphology of fibrous material with needle-like and belt-like became more uniform, the diameter and length were in the range of 50–200 nm and 1–5 μm, respectively. It is obvious that micro morphology of $Mg_2B_2O_5$ one-dimensional nanomaterials is different using ternary molten salts process from single molten process, as shown in Fig. 9. It was reported that the micro

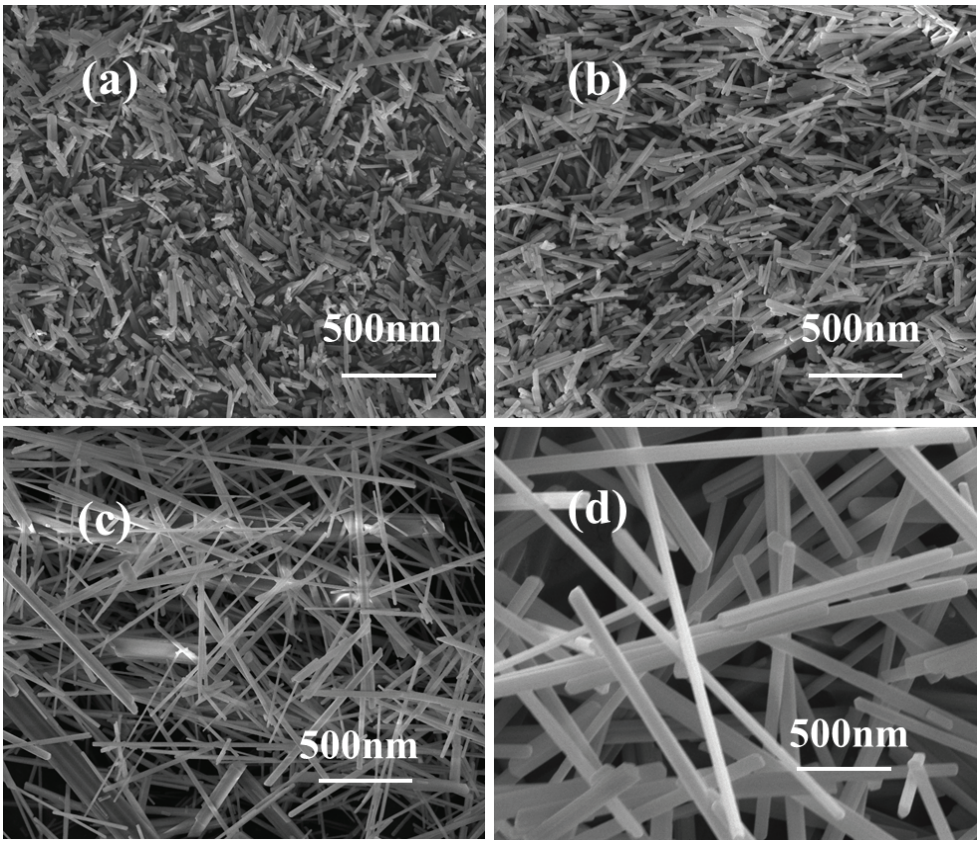

Fig. 8. SEM images of $Mg_2B_2O_5$ nanorods calcined at different temperatures by single molten salt method. (a) 750°C, (b) 770°C, (c) 800°C and (d) 820°C.

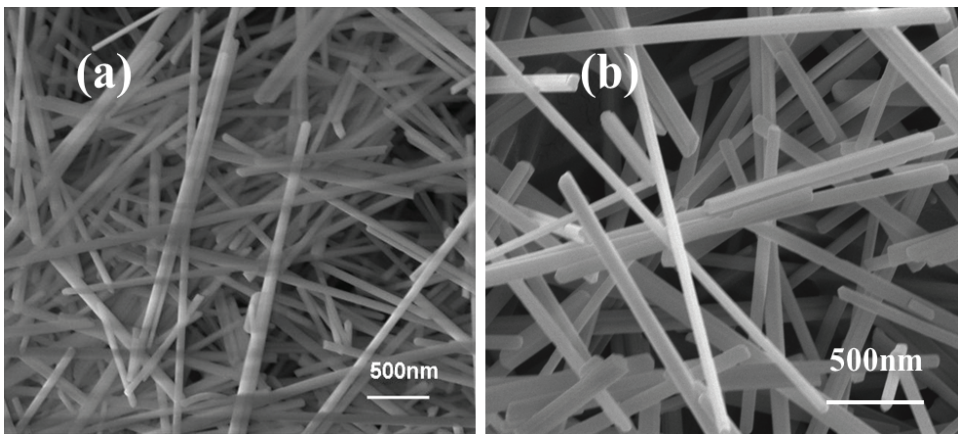

Fig. 9. SEM images of $Mg_2B_2O_5$ nanorods using different methods: (a) ternary molten salts method and (b) single molten salt method.

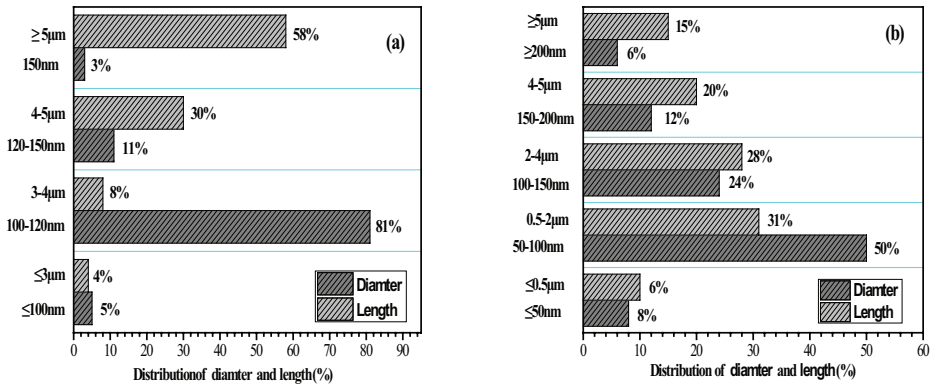

Fig. 10. Size distribution of $Mg_2B_2O_5$ nanorods (a) ternary molten salts method at 780°C for 2 h and (b) single molten salt method at 820°C for 2 h.

morphology of powder has related to the solubility of solutes in molten salt, its core content is that if the solubility of solutes are similar in the molten salt, new compounds were directly produced, or otherwise the larger one will diffuse to the surface of the small one and new compounds were produced. In this paper, it is deduced that the solubility of $Mg_2(OH)_3Cl$ and $Na_2B_4O_5(OH)_4{\cdot}8H_2O$ is different in KCl-NaCl-Na_2SO_4 and NaCl molten salts, which lead to different micro morphology. In the single molten salt, Cl^- made (110) lattice plane grow fast and form needle-like and belt-like nanomaterials, SO_4^{2-} made (-210) lattice plane grow fast and form rod-like nanomaterials.

The following micro morphology size distribution of $Mg_2B_2O_5$ one-dimensional nanomaterials further confirmed that it is more uniform using ternary molten salts process than single molten process. Fig. 10(a) shows size distribution of $Mg_2B_2O_5$ nanorods using ternary molten salts method at 780°C for 2 h. The statistical datum indicated that the diameter mainly distributed in the range of 100–150 nm, in which 81% of the particles diameter was between 100 and 120 nm, and 58% of the particles length was more than 5 μm. Fig. 10(b) shows size distribution of $Mg_2B_2O_5$ nanorods using single molten salt method at 820°C for 2 h. It can be seen that the diameter distribution is in the range of 50–200 nm, in which 50% of the particles diameter was between 50 and 100 nm, and 79% of the particles length was in the range of 0.5–5 μm. Compared with single molten salt method, ternary molten salts process was more efficient to form $Mg_2B_2O_5$ nanorods under lower temperature; it not only decreased the calcination temperature but also made the morphology more uniform. It is because that the reaction constituents show good dissolving and migration ability in ternary molten salts and therefore the formation speed of the $Mg_2B_2O_5$ crystals was significantly improved. Furthermore, complex ions were formed in ternary molten salts during calcination process, which played a positive role for reducing the molten salts temperature and diffusion resistance.

Besides, it is reported that with the increased need of water resource, desalination of seawater accounts for worldwide water production, the discharge of concentrated seawater is a key issue, which may cause negative impact on marine environment [22,23], so the process in this paper not only reduces environmental pollution but also turns the magnesium in concentrated seawater into high value products instead of the primary industrial raw materials, advantage significantly.

4. Conclusions

In summary, we successfully prepared $Mg_2B_2O_5$ nanorods by ternary molten salts process using concentrated seawater. The as-prepared nanorods showed a diameter of 100–150 nm and the length of more than 5 μm when calcined at 780°C for 2 h. The calcination temperature of $Mg_2B_2O_5$ nanorods using ternary molten salts method was 40°C lower than single molten salts method in the present study, and the morphology was even more uniform. The ternary molten salts method developed in this study is facile and cost-effective, it could make full use of desalinated concentrated seawater and may be helpful to explore the commercial application potential.

Acknowledgements

This work was supported by the Fundamental Research Funds for the Central Public Welfare Scientific Institution (No. K-JBYWF-2017-T05).

References

[1] C.Q. Hu, Z.H. Gao, X.R. Yang, Fabrication and magnetic properties of Fe_3O_4 octahedra, Chem. Phys. Lett., 429 (2006) 513–517.
[2] W.C. Zhu, G.D. Li, Q. Zhang, L. Xiang, S.L. Zhu, Hydrothermal mass production of $MgBO_2(OH)$ nanowhiskers and subsequent thermal conversion to $Mg_2B_2O_5$ nanorods for biaxially oriented polypropylene resins reinforcement, Powder Technol., 203 (2010) 265–271.
[3] Z.S. Hu, R. Lai, F. Lou, L.G. Wang, Z.L. Chen, G.X. Chen, J.X. Dong, Preparation and tribological properties of nanometer magnesium borate as lubricating oil additive, Wear, 252 (2002) 370–374.
[4] Y. Zeng, H.B. Yang, W.Y. Fu, L. Qiao, L.X. Chang, J.J. Chen, H.Y. Li, M. Zhu, G.T. Zou, Synthesis of magnesium borate ($Mg_2B_2O_5$) nanowires, growth mechanism and their lubricating properties, Mater. Res. Bull., 43 (2008) 2239–2247.
[5] E.G. Baker, Boron zinc oxide and boron magnesium oxide catalysts for conversion hydrocarbons, US Patent, 2889266, 1959.
[6] A.F. Qasrawi, T.S. Kayed, A. Mergen, M. Gürü, Synthesis and Characterization of $Mg_2B_2O_5$, Mater. Res. Bull., 40 (2005) 583–589.
[7] P.W. Ranby, Titanium Activated Magnesium Borate, US Patent, 2758094, 1956.
[8] D.I. Shahare, S.J. Dhoble, S.V. Moharil, Preparation and characterization of magnesium-borate phosphor, J. Mater. Sci. Lett., 12 (1993) 1873–1874.

[9] C. Furetta, G. Kitis, P.S. Weng, T.C. Chu, Thermoluminescence characteristics of MgB_4O_7: Dy, Na, Nucl. Instrum. Methods Phys. Res., Sect. A: Accel. Spectrom, Detect. Assoc. Equip., 420 (1999) 441–445.
[10] Y. Li, Z.Y. Fan, J.G. Lu, R.P.H. Chang, Synthesis of magnesium borate ($Mg_2B_2O_5$) nanowires by chemical vapor deposition method, Chem. Mater., 16 (2004) 2512–2524.
[11] J. Zhang, Z.Q. Li, B. Zhang, Formation and structure of single crystalline magnesium borate ($Mg_3B_2O_6$) nanobelts, Mater. Chem. Phys., 98 (2006) 195–197.
[12] R.Z. Ma, Y. Bando, D. Golberg, T. Sato, Nanotubes of magnesium borate, Angew. Chem. Int. Ed., 42 (2003) 1836–1838.
[13] B.S. Xu, T.B. Li, Y. Zhang, Z.X. Zhang, X.G. Liu, J.F. Zhao, New synthetic route and characterization of magnesium borate nanorods, Cryst. Growth Des., 8 (2008) 1218–1222.
[14] A.M. Chen, P. Gu, Z.M. Ni, 3D flower-like magnesium borate microspheres assembled by nanosheets synthesized via PVP-assisted method, Mater. Lett., 68 (2012) 187–189.
[15] J.W. Jiang, L. Wang, Q. Yang, D.R. Yang, Synthesis of magnesium borate nanorods by sol-gel process, J. Inorg. Mater., 21 (2006) 833–837.
[16] X.C. Liu, Molten Salt Synthesis of $ZnTiO_3$ Powders with round 100 nm grain size crystalline morphology, Mater. Lett., 80 (2012) 69–71.
[17] S. Li, X. Fang, J. Leng, H.Z. Shen, Y. Fan, D.P. Xu, A new route for the synthesis of $Mg_2B_2O_5$ nanorods by mechano-chemical and sintering process, Mater. Lett., 64 (2010) 151–153.
[18] W.C. Zhu, Q. Zhang, L. Xiang, F. Wei, X.T. Sun, X.L. Piao, S.L. Zhu, Flux-assisted thermal conversion route to pore-free high crystallinity magnesium borate nanowhiskers at a relatively low temperature, Cryst. Growth Des., 8 (2008) 2938–2945.
[19] W.C. Zhu, Q. Zhang, L. Xiang, S.L. Zhu, Repair the pores and preserve the morphology: formation of high crystallinity 1D nanostructures via the thermal conversion route, Cryst. Growth Des., 11 (2011) 709–718.
[20] W.C. Zhu, R.G. Wang, S.L. Zhu, L.L. Zhang, X.L. Cui, H. Zhang, X.L. Piao, Q. Zhang, Green, noncorrosive, easy scale-up hydrothermal-thermal conversion: a feasible solution to mass production of magnesium borate nanowhiskers, ACS Sustain. Chem. Eng., 2 (2014) 836–845.
[21] X.T. Tao, X.D. Li, Catalyst-free synthesis, structural, and mechanical characterization of twinned $Mg_2B_2O_5$ nanowires, Nano Lett., 8 (2008) 505–510.
[22] P. Palomar, I.J. Losad, Desalination in Spain: Recent developments and recommendations, Desalination, 255 (2010) 97–106.
[23] L. Sabine, H. Thomas, Environmental impact and impact assessment of seawater desalination, Desalination, 220 (2008) 1–15.